Numerical Modelling of Load Bearing Steel Stud Walls under Fire Conditions

S. Gunalan
PhD Researcher, Queensland University of Technology, Brisbane, Queensland, Australia

M. Mahendran
Professor, Queensland University of Technology, Brisbane, Queensland, Australia

ABSTRACT: Fire design is an essential part of the overall design procedure of structural steel members and systems. Conventionally, increased fire rating is provided simply by adding more plasterboards to Light gauge Steel Frame (LSF) stud walls, which is inefficient. However, recently Kolarkar & Mahendran (2008) developed a new composite wall panel system, where the insulation was located externally between the plasterboards on both sides of the steel wall frame. Numerical and experimental studies were undertaken to investigate the structural and fire performance of LSF walls using the new composite panels under axial compression. This paper presents the details of the numerical studies of the new LSF walls and the results. It also includes brief details of the experimental studies. Experimental and numerical results were compared for the purpose of validating the developed numerical model. The paper also describes the structural and fire performance of the new LSF wall system in comparison to traditional wall systems using cavity insulation.

1 INTRODUCTION

Light Gauge Steel Framing (LSF) load bearing stud wall systems are made of cold-formed and thin-walled steel lipped channels. Under fire conditions, these thin-walled sections heat up quickly resulting in fast reduction to their strength and stiffness. Innovative fire protection systems are therefore essential without simply adding on more plasterboards. According to Feng et al. (2003a), the cavity insulation was found to be improving the fire resistance of steel stud wall panels. However, in the studies of Kodur & Sultan (2001) and Alfawickhari (2001), LSF wall assemblies without cavity insulation provided higher fire resistance in comparison to cavity insulated assemblies. Recently Kolarkar & Mahendran (2008) developed a new composite panel system (Fig. 1), where the insulation was placed outside the steel frame. They found that the fire resistance of LSF walls improved considerably. However, their study was limited to fire tests with an applied axial compression load of 0.2 x ambient temperature ultimate capacity, ie. a load ratio of 0.2. Hence a further experimental study with a higher load ratio of 0.4 and a numerical study of LSF stud walls were undertaken under fire conditions. Experimental results were used to validate the developed numerical model. This paper presents the details of the experimental and numerical studies, which were carried out to investigate the structural and fire performance of load bearing steel stud wall assemblies using the new composite panel system under different load ratios.

2 EXPERIMENTAL STUDY

2.1 *Test specimens*

Three LSF wall specimens of dimensions 2.1m width x 2.4m height were built using the new composite panels and tested under fire conditions. The test steel frame was made using four lipped channel section studs that were attached to the top and bottom tracks made of unlipped channel sections. All the studs and tracks used were fabricated from 1.15 mm G500 steel sheets (minimum specified yield strength of 500 MPa). The composite panels were made of two 16 mm plasterboards attached using screws with rock fibre or glass fibre insulation sandwiched between them, and were attached on both sides of the steel wall frame (Figs. 1 and 2).

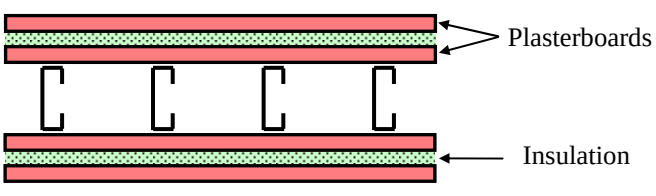

Figure 1. LSF stud walls using the new composite panel

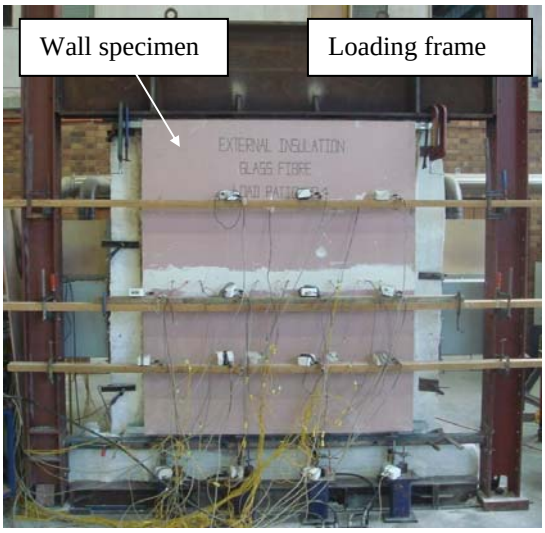

Figure 2. Test specimen before testing

2.2 *Test set-up and procedure*

The target axial compression load was applied first and maintained throughout the fire test. A gas furnace was then used to expose one side of the wall to the standard temperature-time fire curve. Figure 2 shows the test specimen before testing. Further details can be found in Gunalan (2010).

2.3 *Test observations and results*

Test LSF walls deformed towards the furnace as a result of thermal bowing and their strength was reduced due to heating. Eventually they could not support the applied load and collapsed after a period of exposure to fire. The exposed plasterboards were found to be considerably damaged, but had not completely fallen off. They were stripped off and the debris removed to expose the frame. Local buckling deformations along the studs were noted, which confirmed the occurrence of local buckling of studs before the ultimate failure.

Table 1. Structural response of test specimens

Test	Configuration	Insulation type	Insulation location	Load ratio	Failure time (min.)
1		Glass Fibre	External	0.2	118
2		Glass Fibre	External	0.4	108
3		Rock Fibre	External	0.4	134
1*		None	-	0.2	111
2*		Glass Fibre	Cavity	0.2	101
3*		Rock Fibre	Cavity	0.2	107
4*		Rock Fibre	External	0.2	136

* Tests conducted by Kolarkar (2010)

Table 1 gives the fire resistance ratings of the LSF wall specimens tested under a constant axial compression load (load ratios of 0.2 and 0.4) during the fire tests of this study (Tests 1 - 3). It also includes the results of some of the tests conducted by Kolarkar (2010) for the purposes of comparison (Tests 1* - 4*). These tests included one specimen without cavity insulation and composite panel, and some specimens with cavity insulation (see Table 1). These results confirm the superior performance of LSF walls using external insulation over cavity insulation. For example, Tests 1 and 4* gave about 20% increase in fire rating compared to Tests 2* and 3* for a load ratio of 0.2. On the other hand, Test 1* without any cavity insulation gave higher fire ratings than Tests 2* and 3* with cavity insulation. The results with cavity insulation is inferior to no insulation case due to high temperature gradient.

3 FINITE ELEMENT MODELLING

3.1 *Basic parameters*

LSF studs are made of thin cold-formed sheets. In finite element modelling this can be represented using shell elements. Kaitila (2002) and Feng et al. (2003b) used S8R5 and S4R elements in their numerical studies, respectively. In the current study, S4R element type was selected since it provides similar results as S4 elements with less memory space and time. This element type ensured sufficient degrees of freedom for buckling deformations of light gauge cold-formed steel compression members.

The use of a finer finite element mesh will produce more accurate results. However, it may not give the most economical simulation since it needs more processing time and memory. Therefore the optimum size of the element was found to be 4 mm x 4 mm based on a convergence study.

In order to simulate fire tests accurately, the mechanical properties used in finite element analyses (FEA) should be the same as those of test specimens. Therefore the measured values of elastic modulus and yield strength reported in Kolarkar (2010) were used in FEA. These measured yield strength and modulus of elasticity values were 569 MPa and 213520 MPa, respectively. The mechanical properties significantly influence the elastic buckling and ultimate strength behaviour of LSF steel studs at elevated temperatures because they deteriorate with increasing temperatures. Kankanamge (2010) undertook a study to investigate the mechanical properties of cold-formed steels at elevated temperatures and developed suitable predictive equations. These equations were used in the FEA of this study. The coefficient of thermal expansion was taken as a constant value of 0.000014 $°C^{-1}$ while the Poisson's ratio was assumed as 0.3.

3.2 *Boundary conditions*

For an accurate simulation of test specimens, appropriate boundary conditions must be included. Based on previous studies (Kaitila, 2002) and experimental observations, only the individual stud was considered in the finite element models by taking into account the appropriate loading and boundary conditions as shown in Figure 3.

In the numerical study of Kaitila (2002), the studs were considered to be pin-ended. Rigid end plates were used at each end. Zhao et al. (2005) considered two support conditions. The first one was hinged at both ends while the second one was fixed at one end and hinged at the other end. Both ends were modelled using rigid end plates. Feng et al. (2003b) used one rigid plate at each end of the column. Two horizontal restraints were applied at the centroid of the channel section at each end.

In our experimental study, the end support conditions were maintained as pinned connections. Hence this numerical study also used pinned support conditions. Rigid plates made of R3D4 elements were attached to each end of the stud, and twisting (ROTX) was restrained. The ends of the stud were restrained in the two major axis directions (UY and UZ). The axial displacement (UX) was restrained at one end of the member. An axial compressive load was applied at the centroid of the other end.

The simulation of plasterboard support plays a major role in the FEA of LSF studs. In the current study, the load carrying capacity of plasterboards was ignored. However, the lateral restraint provided by this lining material was taken into account. The connection of steel stud with plasterboard was represented by a suitable boundary condition restraining the lateral displacement of both flanges at 300 mm intervals. This boundary condition was applied to both flanges along the length as shown in Figure 3.

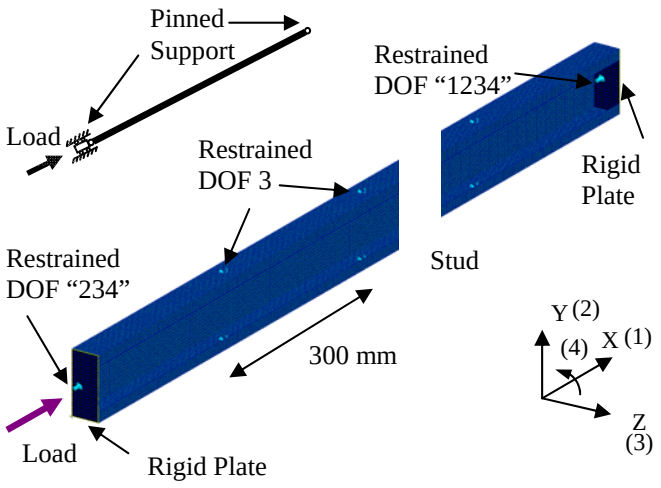

Figure 3. Loading and boundary conditions used in FEA

3.3 *Initial imperfections and residual stresses*

Kaitila's (2002) model included both local and global initial imperfections. Zhao et al. (2005) and Feng et al. (2003b) used 1 mm and L/1000, respectively, as their amplitudes of initial imperfections. However, due to the dominance of thermal bowing the effect of initial imperfections does not have any significant effect on the behaviour of LSF studs at elevated temperatures. In the finite element analyses of studs under fire conditions, the first step was an eigen buckling analysis at ambient conditions, in which the buckling modes are obtained and the deflection profile of the lowest buckling mode was used to input the initial imperfections. A value of b/150 was used in this model as the amplitude.

At higher temperatures, the effect of residual stresses is negligible. Therefore they were neglected in this model as was done in past research.

3.4 *Temperature distribution*

In order to simulate the fire tests, it was decided to use the measured temperature profiles from the fire tests. However, at any time during the analyses, the non-uniform temperature field in the cross-section of a column was simplified by assuming uniform temperatures in the flanges and lips on both the fire and cold sides. A linear temperature distribution was assumed for the web as shown in Figure 4. The average measured temperature profiles across the stud cross-section from Test 1 are shown in Figure 5.

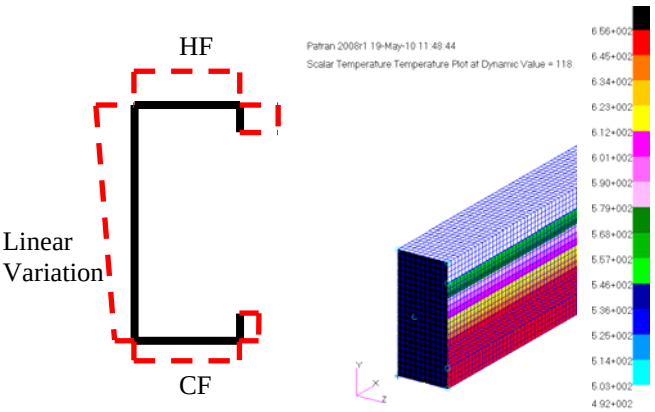

Figure 4. Simplified temperature distribution used in FEA

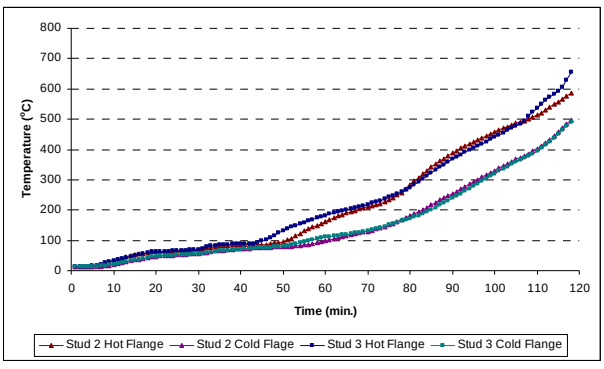

Figure 5. Average temperature profiles used in FEA of Test 1

3.5 *Finite element analysis procedure*

Finite element analysis of LSF stud walls under fire conditions can be undertaken under two conditions, namely steady and transient state conditions. In the case of steady state conditions, the temperature distributions in the stud cross-section are raised to the target levels and then maintained. The load is then applied in increments until failure. In the case of transient state conditions, the load is applied in increments until it reaches the target load (a particular load ratio). Thereafter the temperature distribution is input in a time frame until failure. Feng et al. (2003) used steady state modelling whereas Kaitila (2002) and Zhao et al. (2005) used transient modelling in their numerical analyses.

Full scale fire tests were similar to that of transient state modelling. In order to simulate fire tests, it is important to model the complete loading history in a realistic way. Therefore finite element analyses should be performed under transient state conditions where the stud was subjected to a pre-determined axial load while exposing them to the measured temperature profiles. On the other hand, in order to develop design rules, the load carrying capacity of studs has to be determined for a given temperature profile. In this case the analyses should be performed under steady state conditions where the stud is subjected to a pre-defined temperature profile and then the load is applied incrementally until it fails. In this case, several analyses should be undertaken in closer time intervals to simulate experiments. In this numerical study both types of analyses were conducted using the measured temperature profiles from Kolarkar (2010) and the current experimental study.

3.5.1 *Transient state analyses*

In the transient state analysis, each finite element analysis was performed in three steps. The first step was an eigen buckling analysis at ambient conditions from which the buckling modes were obtained and the deflection profile of the lowest buckling mode was used to input the initial imperfections. In the second and third steps, load and temperatures were applied one after the other and nonlinear analyses were undertaken. For example, the measured temperature distribution shown in Figure 5 was used in FEA of Test 1 studs under transient conditions. Linear variation was assumed for the web from hot flange temperature to cold flange temperature. The lips are assumed to be at the same temperature as their corresponding flanges. The analysis was conducted in a time frame to obtain a deformation curve for each test. The accuracy of the developed finite element models were validated using experimental deformation curves of LSF studs.

3.5.2 *Steady state analyses*

The finite element analyses were conducted under steady state conditions to confirm the failure time obtained under transient state conditions. In addition to this, it is convenient to compare these results (failure loads obtained from FEA under steady state conditions) with design capacity calculations.

Each finite element analysis under steady state conditions was also performed in three steps. The first step was an eigen buckling analysis at ambient condition, in which the buckling modes were obtained and the deflection profile of the lowest buckling mode was used to input the initial imperfections. In the second and third steps, temperatures and load were applied one after the other and nonlinear analyses were performed for them.

The model under steady state conditions was created similar to that under transient conditions. However, the method of analyses was different. First the temperature distributions in the steel cross section were raised to the target levels and maintained. Afterwards the load was applied in increments until failure. The steel stud temperatures were based on the average temperature distribution for the critical stud obtained from the experimental study.

The analysis was conducted in a time frame to obtain the ultimate loads of stud, and hence load ratio curves versus time and temperature were obtained for each test. In this case, the average hot flange temperature was used. The accuracy of the developed finite element models were validated using the experimental failure times of LSF walls.

4 RESULTS AND DISCUSSIONS

4.1 *Transient state analyses*

Figures 6 and 7 show the axial deformation and lateral deflection of two central studs in the LSF walls with time from experiments and FEA under transient conditions. The agreement of these curves is very good compared to the previous numerical studies of LSF walls under fire conditions. Any difference may be due to the approximations in the assumed temperature distributions used in FEA.

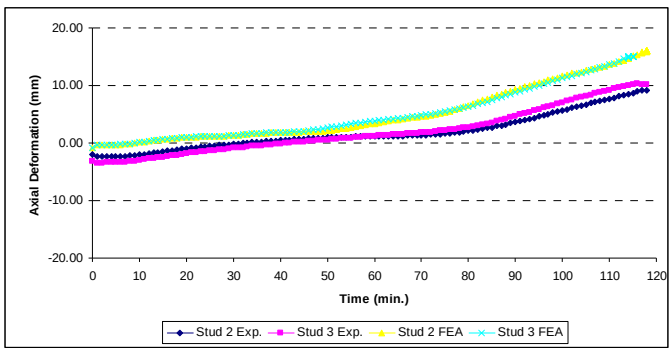

Figure 6. Axial deformations versus time

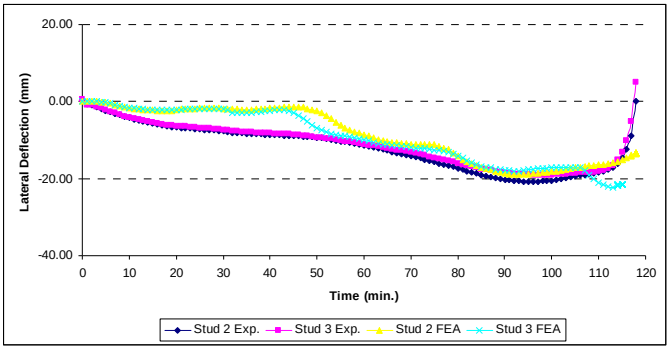

Figure 7. Lateral deflections versus time

Figure 8 shows the failure modes obtained from fire tests and FEA. In one of the tests the stud failure was towards the furnace and at other times it was away from the furnace. However in FEA it always failed towards the furnace. This may be due to the omission of any loading eccentricity in FEA. Thermal bowing deformations in the fire tests are likely to induce an eccentric loading towards the hot side. This eccentric loading and the effect of neutral axis shift will cause a stud to reverse its initial movement towards the furnace. Therefore during the final stages of the fire tests, there is a possibility for the studs to bend away from the furnace for most of the tests. However this eccentric loading was not considered in FEA and this resulted in failures towards the furnace due to temperature gradient in all the test simulations.

Both tests and FEA showed the occurrence of local buckling in the stud near failure. In Test 1, the stud was found to have crushed in the middle at failure after 118 minutes. This could not be achieved in FEA when it ended after 115 minutes. However, this failure time obtained from FEA under transient conditions was confirmed by the corresponding FEA under steady state conditions. This confirms that both the transient and steady state methods can be used to model the LSF studs restrained by plasterboards under fire conditions.

Figure 8. Failure modes obtained from FEA and Test 1

4.2 *Steady state analyses*

The FEA results under steady state conditions can be used to plot the ultimate load capacity of stud expressed as a load ratio against time. Figure 9 shows the variation of load ratio with time based on the average temperatures along the stud whereas Figure 10 shows the variation of load ratio with respect to hot flange temperatures. These useful plots were developed for LSF walls without cavity insulation (2x2), with cavity rock fibre or glass fibre insulation (CI-RF, CI-GF) and composite panels with rock fibre and glass fibre insulation (CP-RF, CP-GF) as shown in Figures 9 and 10. Feng et al. (2003b) also obtained similar curves for their LSF panels.

A small reduction in the load ratio was experienced even for lower temperatures in the range of 100-300^{o}C, where there is no reduction in steel yield stress. This is mainly due to two factors. Firstly, the elastic modulus is reduced at these temperatures and this reduces the stiffness of the steel stud. Secondly, in this phase, the stud experienced greater temperature deviation across the stud. This will result in more lateral deflections and hence a larger bending moment will be induced in the stud. These effects caused the reduction in load ratios even at temperatures below 300^{o}C.

There is a large variation in the load versus time graphs for all the tests due to the variation in the assumed temperature distribution. However, the load ratio versus temperature graphs were almost the same for all the panels, ie. the failure temperature of the stud is about the same for a given load ratio for all the specimens. This means that structurally similar studs will fail at the critical failure temperature regardless of the number of plasterboards and insulation types used. The effect of plasterboards and cavity/external insulation is simply to delay the time to reach that critical temperature in the steel stud. This also means importantly that the lateral restraint provided by one or two plasterboards is about the same.

In all the tests and FEA, the specimens failed at about 600^{o}C when they were subjected to a load ratio of 0.2. The failure temperature of specimens was about 520^{o}C for an increased load ratio of 0.4. This shows that the current limiting temperature method of using 400^{o}C as a benchmark is too conservative and will lead to very conservative fire designs.

Table 2 compares FEA predicted failure times with those obtained from fire tests. The FEA results agreed well with the fire test results when average temperatures along the stud were used. Except the composite panel with rock fibre insulation, the failure time of all other LSF wall specimens were predicted within an error of 5 minutes, which is a considerable improvement compared to past researches in this field. The composite panel with rock fibre as insulation failed earlier in the test than expected.

This was due to the insufficient space for expansion between the loading frame and the panel.

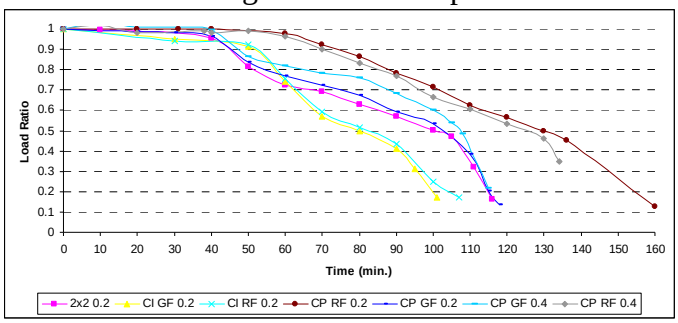

Figure 9. Variation of Load Ratio with Time

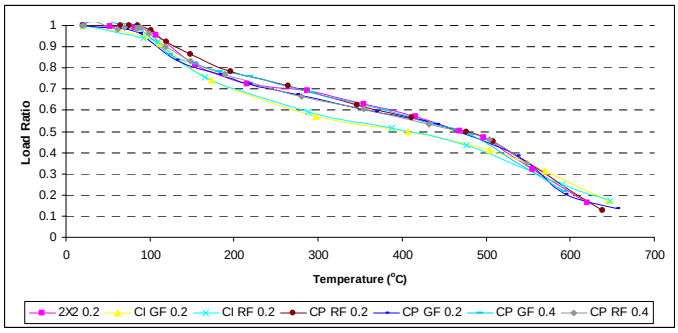

Figure 10. Variation of Load Ratio with Temperature

Table 2. Failure times predicted by FEA

Test	Configuration	Insulation type	Load ratio	Failure time (min.)	
				Experiment	FEA
1		Glass Fibre	0.2	118	115
2		Glass Fibre	0.4	108	110
3		Rock Fibre	0.4	134	132
1*		None	0.2	111	115
2*		Glass Fibre	0.2	101	100
3*		Rock Fibre	0.2	107	104
4*		Rock Fibre	0.2	136	155

* Tests conducted by Kolarkar (2010)

5 CONCLUSIONS

This paper has described an investigation into the structural and fire performance of a new LSF wall system based on numerical and experimental studies. Suitable finite element models were developed and analysed under both steady and transient state conditions. The use of accurate numerical models as described in this paper allowed the inclusion of various complex thermal and structural effects such as thermal bowing, local buckling and shift of neutral axis at elevated temperatures. Developed numerical models were validated by comparing with corresponding fire test results. Importantly the numerical studies confirmed the fire rating improvements offered by the new composite panel system.

6 ACKNOWLEDGEMENTS

The authors wish to thank Australian Research Council for the financial support to this project through the Discovery Grants Scheme, QUT for providing the required experimental and computing facilities and technical support, and Boral and Fletcher Insulation for providing the required plasterboard and insulation materials. Fire test results from Prakash Kolarkar are also acknowledged.

7 REFERENCES

Alfawakhiri, F. 2001. Behaviour of cold-formed-steel-framed walls and floors in standard fire resistance tests. PhD thesis, Carleton University, Ottawa, Ontario, Canada.

Dolamune Kankanamge, N. 2010. Structural behaviour and design of cold-formed steel beams at elevated temperatures. PhD Thesis, QUT, Brisbane, Australia.

Feng, M. Wang, Y.C. & Davies, J.M. 2003a. Thermal performance of cold-formed thin-walled steel panel systems in fire. *Fire Safety Journal* 38, pp. 365-394.

Feng, M, Wang, Y.C. & Davies, J.M. 2003b. Axial strength of cold-formed thin-walled steel channels under non-uniform temperatures in fire. *Fire Safety Journal* 38, pp. 679-707.

Gunalan, S. 2010. Structural behaviour and design of a new light gauge cold-formed steel stud wall system under fire conditions. PhD Thesis, QUT, Brisbane, Australia, In preparation.

Kaitila, O. 2002. Finite Element Modelling of Cold-formed Steel Members at High Temperatures. Masters Thesis, HUT, Otakaari, Finland.

Kodur, V.R. & Sultan, M.A. 2001. Factors governing fire resistance of load-bearing steel stud walls. *Proceeding of the 5th AOSFST International Conference*, Newcastle, Australia, pp. 1–2.

Kolarkar, P.N. & Mahendran, M. 2008. Thermal performance of plasterboard lined steel stud walls. *Proceeding of the 19th International Specialty Conference on Cold-Formed Steel Structures*, St. Louis, Missouri, USA, pp. 517-530.

Kolarkar, P.N. 2010. Fire performance of plasterboard lined steel stud walls. PhD Thesis, QUT, Brisbane, Australia, In preparation.

Zhao, B. Kruppa, J. Renaud, C. O'Connor, M. Mecozzi, E. Apiazu, W. Demarco, T. Karlstrom, P. Jumppanen, U. Kaitila, O. Oksanen, T. & Salmi. P. 2005. Calculation rules of lightweight steel sections in fire situations. *Technical steel research*, European Commission, Brussels, Belgium.